

α,β -Unsaturated Carbonyl System of Chalcone-Based Derivatives Is Responsible for Broad Inhibition of Proteasomal Activity and Preferential Killing of Human Papilloma Virus (HPV) Positive Cervical Cancer Cells

Martina Bazzaro,^{*,†,◇} Ravi K. Anchoori,^{‡,§,×} Mohana Krishna R. Mudiam,^{§,×} Olga Issaenko,[†] Srinivas Kumar,[§] Balasubramanyam Karanam,[‡] Zhenhua Lin,^{‡,●} Rachel Isaksson Vogel,[∞] Riccardo Gavioli,[⊥] Federica Destro,[⊥] Valeria Ferretti,[#] Richard B. S. Roden,^{‡,§,⊥,◇} and Saeed R. Khan^{*,§,◇}

[†]Masonic Cancer Center and Department of Obstetrics, Gynecology and Women's Health, University of Minnesota Twin Cities, Minneapolis, Minnesota 55455, United States; [‡]Department of Pathology, [§]Department of Oncology, and [⊥]Department of Gynecology and Obstetrics, The Johns Hopkins University, Baltimore, Maryland 21231, United States; [⊥]Department of Biochemistry and Molecular Biology, University of Ferrara, Ferrara, Italy; [#]Department of Chemistry and Center for Structural Diffractometry, University of Ferrara, I-44100, Ferrara, Italy; and [∞]Masonic Cancer Center Biostatistics and Bioinformatics Core, University of Minnesota Twin Cities, Minneapolis, Minnesota 55455, United States. [◇]M.B., R.B.S.R., and S.R.K. contributed equally to this work. [×]R.K.A. and M.K.R.M. contributed equally to this work. [●]Current address: Department of Pathology, Yanbian University College of Medicine and Key Laboratory of Organism Functional Factors of the Changbai Mountain, Ministry of Education, Yanji-City, Jilin-Province, P. R. China.

Received May 14, 2010

Proteasome inhibitors have potential for the treatment of cervical cancer. We describe the synthesis and biological characterization of a new series of 1,3-diphenylpropen-1-one (chalcone) based derivatives lacking the boronic acid moieties of the previously reported chalcone-based proteasome inhibitor 3,5-bis(4-boronic acid benzylidene)-1-methylpiperidin-4-one and bearing a variety of amino acid substitutions on the amino group of the 4-piperidone. Our lead compound **2** (RA-1) inhibits proteasomal activity and has improved dose-dependent antiproliferative and proapoptotic properties in cervical cancer cells containing human papillomavirus. Further, it induces synergistic killing of cervical cancer cell lines when tested in combination with an FDA approved proteasome inhibitor. Exploration of the potential mechanism of proteasomal inhibition by our lead compound using in silico docking studies suggests that the carbonyl group of its oxopiperidine moiety is susceptible to nucleophilic attack by the γ -hydroxythreonine side chain within the catalytic sites of the proteasome.

Introduction

The 26S proteasome is composed of two 19S regulatory subunits (termed “caps”) and one 20S catalytic subunit (referred to as the “proteolytic core”).^{1,2} The targeting of a protein for degradation by the proteasome occurs via its enzymic conjugation to the small protein ubiquitin. Chains of ubiquitin are recognized by the proteasome caps to facilitate the entrance of the targeted protein into the proteolytic chamber wherein the actual degradation occurs. The 20S proteasome comprises four stacked rings: two α - (outer) and two β - (inner) rings. Each β -ring is composed of seven subunits containing three catalytic sites: the β 1 subunit is associated with a peptidylglutamyl peptide hydrolyzing-like (PGPH-like) activity; the β 2 subunit is associated with the trypsin-like activity (T-like); the β 5 subunit is associated with the chymotrypsin-like activity (CT-like). All three proteolytic activities utilize the γ -hydroxyl group of an N-terminal threonine residue within each catalytic site for nucleophilic attack of the α -amine proton donor/acceptor within the targeted protein.³

The polypeptide targets of the proteasome include proteins involved in cell cycle progression, survival, and inflammation, and while the ubiquitin-dependent proteasomal degradation is crucial for both normal and malignant cells, the higher demand for metabolic/catabolic activity associated with the malignant phenotype renders the ubiquitin–proteasome pathway a suitable tool for cancer treatment.^{4,5}

Inhibition of the catalytic activities of the proteasome can be achieved by compounds that covalently bind the N-terminal threonine residue in the catalytic sites of the β -subunits (this includes bortezomib⁶ (PS-341), salinosporamide A⁷ (NPI-0052), and carfilzomib⁸) or by compounds that bind to the catalytic sites of the β -subunits in a noncovalent fashion^{9,10} like in the case of TMC-95A,^{11,12} ritonavir,¹³ and lipopeptides.¹⁴

Undoubtedly, members of both classes have been shown to have potential as antineoplastic agents with bortezomib, a covalent slowly reversible proteasome inhibitor,¹⁵ to be the first FDA approved for the treatment of multiple myeloma and mantle cell lymphoma.¹⁵

Proteasome inhibitors may be particularly efficacious for certain cancers types with critical pathways that are dependent upon proteolytic degradation. Human papillomavirus (HPV¹⁶)

*To whom correspondence should be addressed. For M.B.: (address) Masonic Cancer Center, Room 490, 420 Delaware Street SE, Minneapolis, Minnesota 55455; (phone) 612-6252889; (fax) 612-626-0665; (e-mail) mbazzaro@umn.edu. For S.R.K.: (address) DPQR/CDER/FDA, Room 1012, New Hampshire Avenue, Silver Spring, Maryland; (phone) 301-796-0051; (fax) 703-796-9816; (e-mail) saeed.khan2@fda.hhs.gov.

^aAbbreviations: AcOH, acetic acid; THF, tetrahydrofuran; DCM, dichloromethane; NMM, *N*-methylmorpholine; HPV, human papilloma virus; DMEM, Dulbecco's modified Eagle medium; SFM, serum free medium.

causes 5% of all cancers worldwide, and the actions of only two of its oncoproteins, E6 and E7, are necessary to maintain the transformed state in cervical cancer.¹⁶ Because E6 and E7 oncoproteins target p53 and pRb tumor suppression proteins for proteasomal degradation, proteasome inhibitors may have utility in the treatment of cervical and other HPV-related cancers.^{17–19}

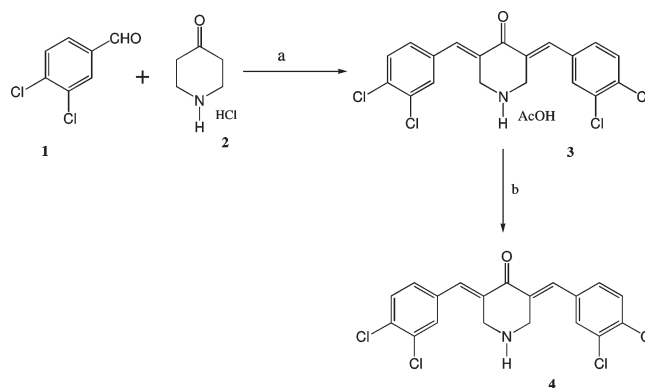
Chalcones (1,3-diphenylpropen-1-ones) are naturally occurring compounds belonging to the flavonoid family and include curcumin and green-tea-derived polyphenols and flavonoids. While several chalcones represent promising tools for cancer treatment,^{20–22} their mechanism of action as antiproliferative and antiangiogenic agents remains unknown. However, recent data suggest that the carbonyl carbon of tea polyphenols and flavonoids confers proteasome-inhibitor properties upon them.^{21,23,24} Herein we report an effort to further optimize the previously described chalcone-based proteasome inhibitor 3,5-bis(4-boronic acid benzylidene)-1-methylpiperidin-4-one (AM-114)²⁰ carrying an α,β -unsaturated carbonyl system and two boronic acid moieties, compound **1**. In here, we describe the synthesis and the biological characterization of a new series of α,β -unsaturated carbonyl system compounds lacking the boronic acid moieties of our previously described proteasome inhibitor and bearing various amino acid substitutions on the amino group of the 4-piperidone. In this new series of compounds, we explore whether the carbonyl group of the α,β -unsaturated system might function as a substrate for the γ -hydroxythreonine side chain within the catalytic sites of the proteasome, as has been previously suggested for curcumin.²³ The amino group of the 4-piperidone is functionalized with either aromatic (compounds **2**, **3**), hydrophobic (compound **4**), acidic (compound **5**), or basic (compound **6**) mono amino acidic substitutions in position P. These mono amino acidic substitutions were chosen because they are predicted to direct the selectivity of proteasome inhibitors toward chymotrypsin-like (compounds **2–4**), peptidylglutamyl peptide hydrolyzing-like (compound **5**), and trypsin-like (compound **6**) activities of the proteasome.^{25,26} In compounds **7–10** the length of the amino acid portion was extended by introduction of dipeptide sequences Phe-Tyr (compound **7**), Glu-Asp (compound **8**), Lys-Arg (compound **9**), and Arg-Lys (compound **10**) to increase the potential affinity of the newly synthesized inhibitors for chymotrypsin-like, peptidylglutamyl peptide hydrolyzing-like, and trypsin-like of the proteasome, respectively, as previously reported.^{25–28}

On the basis of our results, we propose that, unlike our previously identified chalcone-based proteasome inhibitor, the presence of the boronic acid groups is not required for conferring proteasome inhibitory capacity to these new series of compounds and that while the presence of single aromatic amino acid substitution is capable of equally inhibiting the three catalytic activity of the proteasome, the presence of tyrosine or leucine decreases the overall proteasome inhibitor capacity. Further, the combination of our proteasome inhibitor lead compound and the FDA approved proteasome inhibitor bortezomib induces synergistic killing of cervical cancer cell cells. Finally, docking simulation conducted on our new lead compound suggests that the α,β -unsaturated carbonyl system may represent the functional group for nucleophilic attack from the N-terminal threonine residue in the catalytic sites.

Results and Discussion

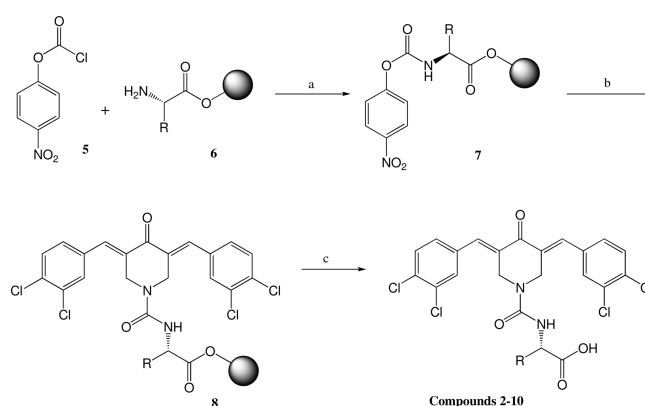
Synthesis. Compounds **2–10** were synthesized following the schematic strategy reported in Schemes 1 and 2 by the

Scheme 1^a



^a Reagents and conditions: (a) dry HCl gas, glacial AcOH, 24 h; (b) triethylamine/dichloromethane.

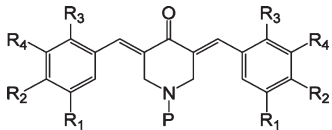
Scheme 2^a



^a Reagents and conditions: (a) DIEA/THF, 0°C to room temp, 45 min; (b) NMM/THF, 0°C to room temp, (c) 20% piperidine–DMF, room temp, 30 min.

classical solution and solid phase reactions. 3,4-Dichlorobenzaldehyde **1** (2.0 mmol) was added to a suspension of 4-piperidone hydrochloride monohydrate **2** (1.0 mmol) in glacial acetic acid (15 mL). Dry hydrogen chloride gas was passed through this mixture for 0.5 h, during which time a clear solution was obtained. After standing at room temperature for 24 h, the precipitate (AcOH salt of bischalcone) was collected and dried under the vacuum. Compound **3** was treated with triethylamine/dichloromethane, and the resultant mixture was stirred for 30 min. Solvents were removed under rotary evaporator and the crude compound was extracted with ethyl acetate/water. The organic layer was washed again with water (50 mL) and evaporated and dried to get bischalcone **4**. *p*-Nitrophenyl chloroformate (10 mmol) and diisopropylethylamine (10 mmol) were added to the amino acid loaded trityl linked polystyrene–1% divinylbenzene resin swollen in THF under nitrogen in a glass vial. After 45 min the resin was washed with THF (3 × 10 mL). Bischalcone **4** (10 mmol) and NMM (10 mmol) in THF were added, and after 16–24 h of stirring a yellow suspension was obtained. After the resin was washed with DCM and methanol each three times, the polymer was dried. The resin bound compounds were cleaved using 20% trifluoroacetic acid in DCM (30 min) and yielded compounds **2–10**. All the compounds were purified by HPLC and characterized by MS and NMR.

Biological Results. To explore the feasibility of the use of new chalcone-based derivatives for the treatment of cervical

Table 1. Summary of the Structure of Compounds 1–10


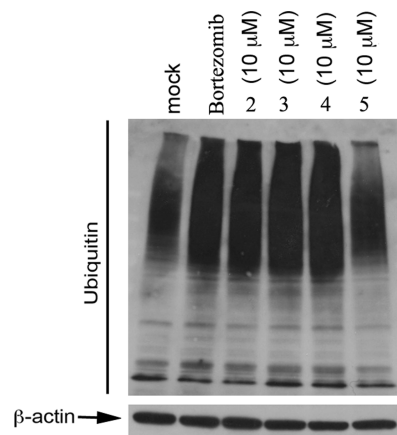
compd	R ₁	R ₂	R ₃	R ₄	P
1	AM-114	H	B(OH) ₂	H	Me
2	RA-1	Cl	Cl	H	-CO-phenylalanine
3	RA-2	Cl	Cl	H	-CO-tyrosine
4	RA-3	Cl	Cl	H	-CO-leucine
5	RA-4	Cl	Cl	H	-CO-glutamic acid
6	RA-5	Cl	Cl	H	-CO-lysine
7	RA-6	Cl	Cl	H	-CO-phenylalanine-tyrosine
8	RA-7	Cl	Cl	H	-CO-glutamic acid-aspartic acid
9	RA-8	Cl	Cl	H	-CO-lysine-arginine
10	RA-9	Cl	Cl	H	-CO-arginine-lysine

Table 2. Cell Killing Activities of Compounds 1–10 on HeLa and CaSki Cervical Cancer Cell Lines^a

compd	IC ₅₀ (μM), HeLa cells	IC ₅₀ (μM), CaSki cells
1	8	9
2	0.32	1.5
3	10	10
4	10	20
5	> 50	> 50
6	> 50	> 50
7	> 50	> 50
8	> 50	> 50
9	> 50	> 50
10	> 50	> 50

^aIC₅₀ values were determined by XTT assay. The IC₅₀ values reported are average of three independent determinations.

cancer, compounds 1–10 (Table 1) were tested for their cell growth inhibitory capacity in the HPV18- and HPV16-positive HeLa and CaSki cervical cancer cell lines in a range of concentrations from 100 to 0.01 μM. The IC₅₀ values by XTT assay in HeLa and CaSki (Table 2) show that compounds 2–4 have an antiproliferative activity that is in the same range of concentrations as our previously reported proteasome inhibitor compound 1, while compounds 5–10 showed a dramatic decrease of the antiproliferative activity with IC₅₀ > 50 μM. Interestingly, compound 2 was 15-fold more potent than compound 1 with IC₅₀ values of 0.32 and 1.5 μM for HeLa and CaSki, respectively. To test whether the decrease in cell viability following exposure to compounds 2–4 was due to perturbation of proteasomal function, we examined the impact of 2–4 treatment on accumulation of polyubiquitinated proteins by immunoblot analysis in HeLa cervical cancer cells. As shown in Figure 1, an 8 h treatment of HeLa cells with compounds 2–4 produced an increase in the levels of polyubiquitinated proteins similar to the one obtained with the FDA approved proteasome inhibitor bortezomib here used as positive control.²⁹ The rapid accumulation of polyubiquitinated proteins observed following exposure to compounds 2–4 is consistent with impairment of proteasomal functions. Notably, no changes in the levels of polyubiquitinated proteins were observed in cells exposed to compound 5, here used as negative control, which also showed IC₅₀ > 50 μM in HeLa and CaSki cell lines. Taken together, these results suggest that the toxicity exerted by compounds 2–4 on cervical cancer cells is associated with in vivo proteasomal inhibition and that

**Figure 1.** Effect of compounds 2–5 treatment on the levels of polyubiquitinated proteins in HeLa cervical cancer cells. Shown are results from immunoblot analysis of ubiquitinated proteins in HeLa cervical cancer cells 8 h after treatment with or without compounds 2–5 at the indicated concentrations. Bortezomib was used as positive control. Equal protein loading in each lane was verified by using an antibody against β-actin.

when tested in the same range of concentrations, compounds that fail to affect cell viability also fail to cause impairment of proteasomal functions. To gain insight on the ability of compounds 2–4 to inhibit specific catalytic subunits within the 20S proteasome, we measured residual fluorogenic activity in 20S purified proteasome pre-exposed to 10 μM 2–4 for 8 h following addition of fluorogenic substrates specific for the three major proteolytic activities of the proteasomes.²⁶ Specifically, compounds 2–4 and the FDA approved proteasome inhibitor bortezomib were tested for their capacity to inhibit the chymotrypsin-like (CT-like), trypsin-like (T-like), and peptidylglutamyl peptide hydrolyzing-like (PGPH-like) activities in vitro of the proteasome purified from lymphoblastoid cell lines (LCLs).³⁰ The profile of proteasome inhibition of compounds 2–4 (Figure 2) shows that 10 μM 2 nearly fully abrogated the CT-like, T-like, and PGPH-like activities of 20S proteasome while compounds 3 and 4 only induced partial inhibition of the CT-like, T-like, and PGPH-like activities with a selective inhibition pattern toward the CT-like activity. The IC₅₀ values are reported in Table 3. The rapid accumulation of polyubiquitinated proteins within 8 h and as early as 2 h (data not shown) observed following compound 2 exposure together with its profile of inhibition on the catalytic subunits of the 20S proteasome suggests that cell death following compound 2 exposure is primarily due to impairment of proteasomal functions. However, to exclude the possibility that lead compound 2 inhibited other proteases, we tested for its capacity to inhibit cathepsin D and calpain in vivo by measuring the residual cathepsin D and calpain activity in HeLa cells exposed to various concentrations of compound 2. We found that 2 had no inhibitory capacity toward cathepsin D or calpain activities when tested at concentrations up to 50 μM (Supporting Information Figure 1). Taken together, these results suggest that while the three-carbon α,β-unsaturated carbonyl carbons system structure may represent the functional group for nucleophilic attack from the N-terminal threonine residue in the catalytic site of the proteasome, the nature of the amino acid inserted in the functionalized amino group of the oxopiperidine plays a role in determining both the potency and the selectivity of this class of compounds. In particular, compound 2 containing the aromatic amino acid

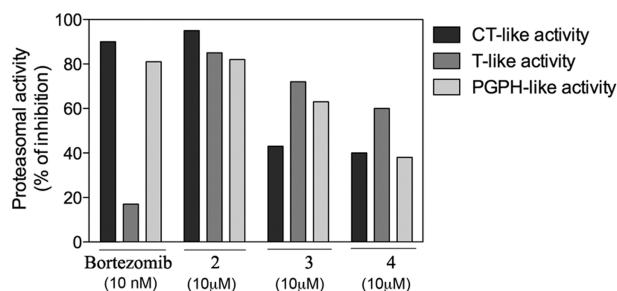


Figure 2. Inhibition of the 20S proteasome activity by compounds 2–4. 20S purified proteasomes were treated for 30 min with or without compounds 2–4 and with positive control at the indicated concentrations following addition of the specific fluorogenic substrates for chymotrypsin-like, trypsin-like, and peptidylglutamyl peptide hydrolyzing-like hydrolytic proteasome capacities. Representative examples of two independent experiments are shown.

Table 3. Inhibition of the Proteolytic Activities of Proteasomes Isolated from LCLs^a

compd	isolated enzyme IC ₅₀ (μM)		
	CT-like	T-like	PGPH-like
2	4.8	6.6	6.2
3	4.2	8.4	> 10
4	9.3	> 10	> 10

^aThe IC₅₀ values reported are the average of three independent determinations.

phenylalanine is capable of equally inhibiting the three catalytic activity of the proteasome (IC₅₀ = 5 μM), while the presence of tyrosine (compound 3) or leucine (compound 4) seems to correspond to a general decrease of proteasomal activity and specifically toward trypsin-like and peptidylglutamyl peptide hydrolyzing-like activities.

The higher demand for metabolic/catabolic activity associated with the malignant phenotype renders proteasome inhibitors a suitable tool for cancer therapy.^{4,5} The toxicity profile observed in the HeLa and CaSki cervical cancer cells following chalcones treatment suggests that the high demand for metabolic activity of highly proliferating cancer cell lines may render them more sensitive to proteasomal inhibition compared to the normal counterpart. To test this hypothesis, the effect on cell viability following lead compound 2 exposure was compared in two additional cervical cancer cell lines SiHa and ME180 versus primary human keratinocytes. As shown in Figure 3, compound 2 treatment produced a dose-dependent drop in the viability of SiHa and ME180 but minimal effects on the viability of primary human keratinocytes. These findings suggested that compound 2 induces dose-dependent cell toxicity in a variety of HPV+ but not in normal cells and that its toxicity may be associated with transformation by HPV, regardless of the oncogenic type (HeLa cells are HPV18+, SiHa and CaSki cells are HPV16+, ME180 cells are HPV58+).

Because our lead compound 2 had a different profile of selectivity toward the catalytic activities of the proteasome compared to bortezomib, we tested whether combination of the latter and compound 2 would be able to generate a broader and therefore more potent inhibition of proteasomal functions compared to single agents alone at lower doses. To test this hypothesis, we utilized the engineered ubiquitin–firefly (Ub-FL) reporter in which four copies of mutant ubiquitin (ubiquitin G76V) are fused to the N-terminus of firefly luciferase (FL).³¹ The Ub-FL and the FL control expression

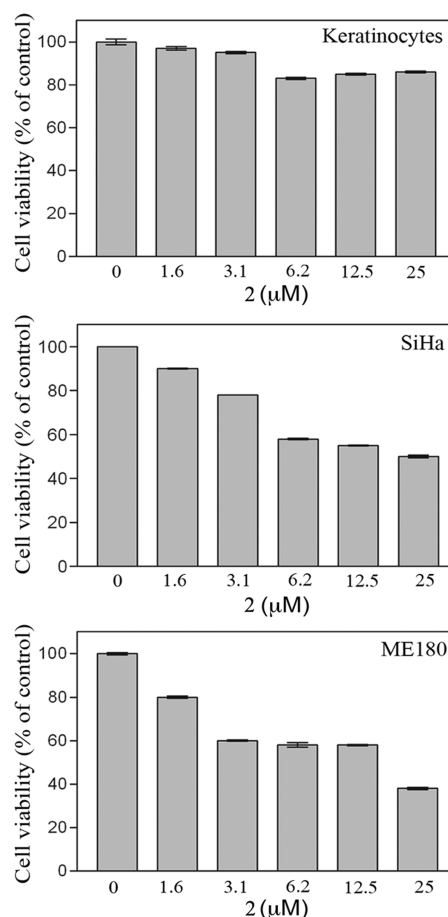


Figure 3. Effect of compound 2 treatment upon cervical cancer cell lines versus normal cells. Cultures of HPV-transformed cervical cancer cells (SiHa and ME180) or primary human keratinocytes were treated with the indicated concentrations of compound 2 for 48 h. Cell viability was determined by XTT assay and plotted as a fraction of the untreated control cultures.

vectors were transiently transfected in HeLa cervical cancer cell line, and expression levels of Ub-FL and FL proteins were confirmed by Western blot analysis (data not shown). After 42 h from transfection, cells were mock-treated or treated with suboptimal doses of bortezomib (5 nM), compound 2 (1 μM), or the combination of both. The results shown in Figure 4 indicate that suboptimal doses of the compounds were able to significantly enhance the stabilization of the Ub-FL decon compared to single agents alone.

Recent studies indicate that inhibition of multiple catalytic activities of the proteasomes by proteasome inhibitors with distinct spectra of activity results in potent antitumor activity at lower and potentially less toxic doses. Because combination of compound 2 and bortezomib triggers a broader and more potent inhibition of proteasomal functions in living cells compared to single agents alone, we tested whether the combination of the latter and compound 2 would induce synergistic killing in HeLa cervical cancer cells. Isobologram analysis (Figure 5) indicates that rather than a simple additive killing the combination is highly synergistic, consistent with inhibition of complementary catalytic functions of the proteasomes. The optimal combination index (CI) was achieved at the following concentrations: (CI = 0.6) bortezomib 3.95 nmol/L per compound 2 2.5 mM/L; (CI = 0.6) bortezomib 6.125 nmol/L per compound 2 1.64 mM/L; (CI = 0.59) bortezomib 7.5 nmol/L per compound 2 1.06 mM/L. We then

wanted to test whether the reduction in the cell viability observed in HeLa cells following exposure to bortezomib and compound **2** alone or in combination was consistent with cell death via apoptosis. To test this hypothesis, HeLa cells were mock-treated or treated with suboptimal doses of bortezomib

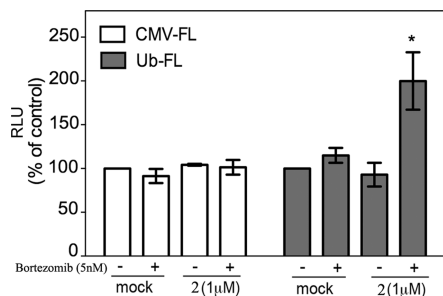


Figure 4. Suboptimal doses of bortezomib and lead compound **2** result in an increased bioluminescence from Ub-FL compared to single agent alone. Transiently transfected firefly luciferase (CMV-FL) and Ub-FL HeLa cervical cancer cells were either mock-treated or treated with bortezomib, lead compound **2**, or a combination at the indicated concentrations for 8 h. Luciferase activity on cell lysate was quantified in relative luminescence units (RLU) and expressed as percent of control. Error bars are standard errors (SE) for three independent experiments.

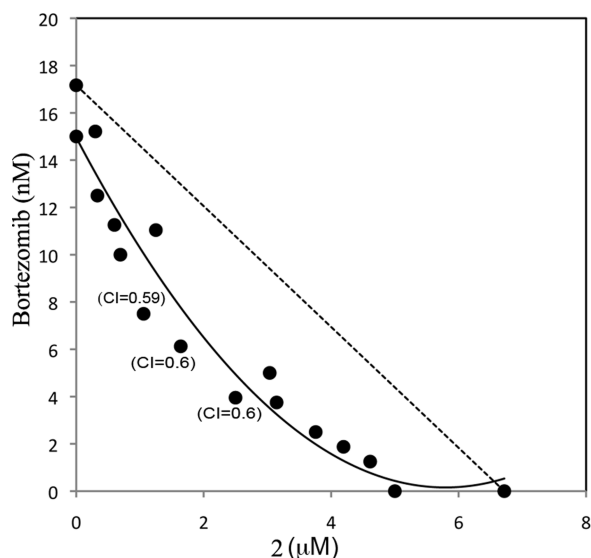


Figure 5. Bortezomib and compound **2** synergistically kill HPV-transformed HeLa cervical cancer cells. HeLa cells were treated with checker board dilution series of bortezomib and lead compound **2**. Cell viability was measured by XTT assay and calculated as percent of control untreated cultures. Synergy is shown by plotting the interaction between drugs in isobologram. The dotted diagonal corresponds to an additive effect, while the points below indicate synergy. CI = combination index.

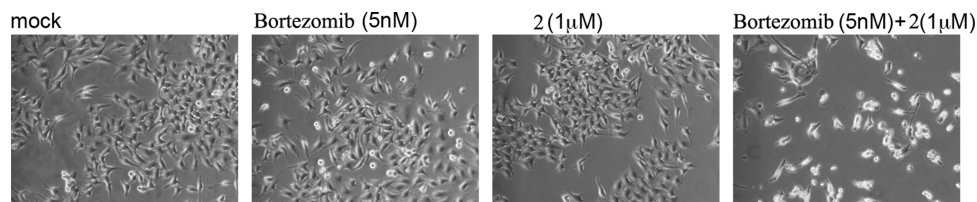


Figure 6. Morphological changes in HeLa cervical cancer cells treated with a combination of bortezomib and lead compound **2**. Shown are the results from phase contrast microscopy of HeLa cultures exposed to bortezomib, compound **2**, or a combination at the indicated concentration for 48 h.

(5 nM), lead compound **2** (1 μ M), or combination of bortezomib (5 nM) + compound **2** (1 μ M) and their morphology was evaluated 48 h after treatment. As shown in Figure 6, combination treatment resulted in greater apoptotic-associated morphological changes in HeLa cells compared to single treatment alone.

In order to obtain a deeper insight into the molecular basis of the enzyme–inhibitor recognition process, the molecule exhibiting the highest affinity, compound **2**, was chosen for performing docking simulations to 20S proteasome, cocrystallized with the β 5-inhibitors homobelactosin C and 2-spiro-lactacystin, whose structures were retrieved from the Protein Data Bank, PDB.³² The lowest unoccupied molecular orbital (LUMO) of compound **2** was found by DFT calculations to be localized mainly around the carbonyl group of the oxopiperidine moiety, as shown in Figure 7A. This finding, according to the fact that a nucleophilic reaction is usually predicted to occur on the atom having the largest LUMO, could be taken as an indication that this group is the most reactive toward an attacking nucleophile. Actually, in the first docking simulation, out of 10 “poses” with high docking scores, 4 have the “active” carbonyl group located at 3–4 Å away from the nucleophilic threonine residue, a distance that is typical of a hydrogen bonding interaction in this type of emulation with rigid protein frame. The pose with the highest score and a schematic view of the ligand–enzyme interaction are reported in Figure 7B and Figure 7C, respectively. The binding pocket appears to have a T shape, resembling the molecule’s conformation. Parts of the inhibitor, i.e., the two chlorine atoms of phenyl A (upper part of Figure 7C) and some of the carbon atoms belonging to the terminal phenyl group C, are placed toward the inner proteasome channel. Many of the amino acid residues, which we suggest, are participating in the formation of the ligand-binding pocket, i.e., Ser129, Gln131, Gly128, Lys33 are found to be involved in homobelactosin-enzyme interactions as well. A π – π short contact (distance between the centroids of the phenyl rings 3.6 Å) was suggested between Tyr168 residue and phenyl group C. Most interestingly, the oxygen of the oxopiperidine was located at a distance of 3.1 Å from the active Thr residue, positioning in this way the carbonyl group in a suitable place to undergo a possible nucleophilic attack. Furthermore, the “docked” compound **2** accommodated in the β 5 binding site of the proteasome/2-spiro-lactacystin structures shows a very similar interaction pattern with the surrounding residues. To better visualize how the present compound could act inside the enzyme, a superposition of the three inhibitors (compound **2**, homobelactosin C, and 2-spiro-lactacystin) is shown in Figure 7D. Compound **2**, although quite different from a chemical point of view, is able to efficiently “occupy” the binding pocket, in particular in proximity of the active threonine

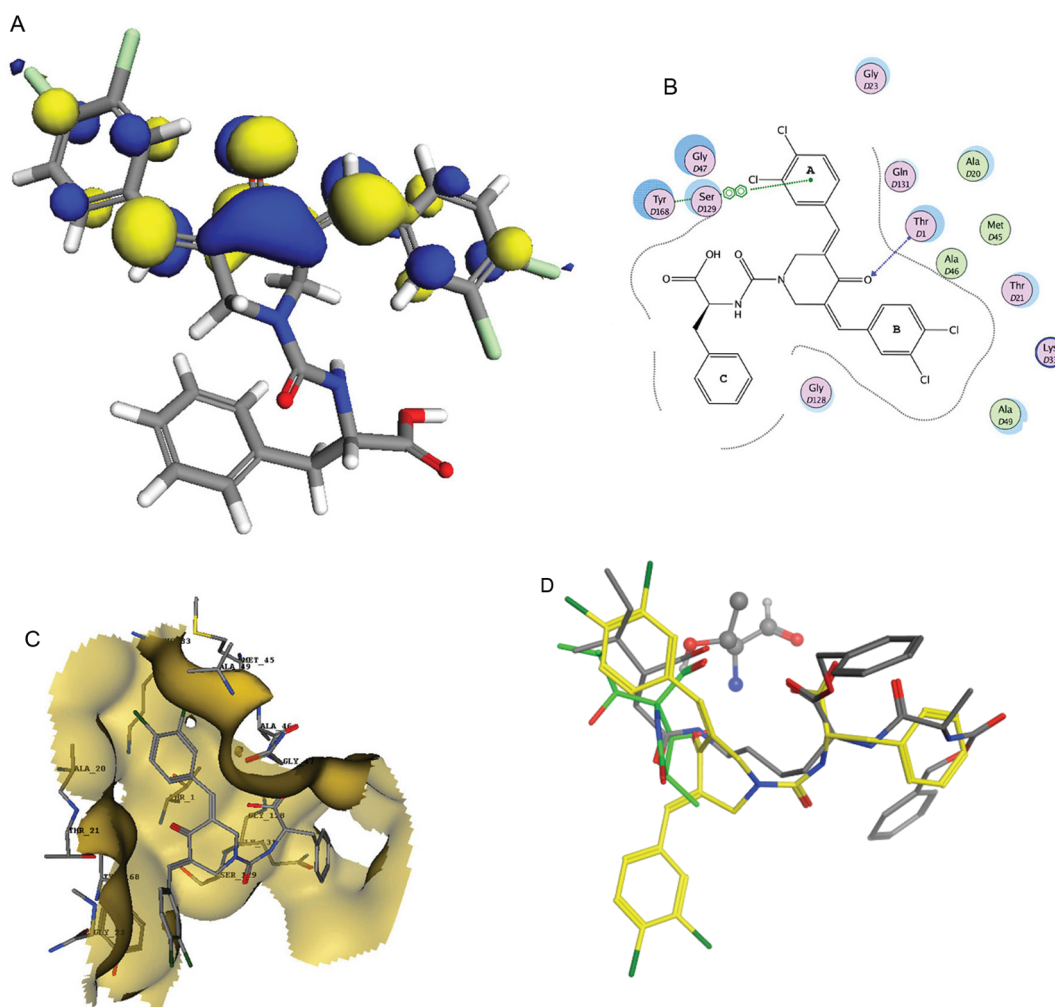


Figure 7. Docking simulation of lead compound **2** to 20S proteasome. (A) LUMO (in blue) is localized around the carbonyl group of the oxopiperidine of lead compound **2**. (B) Schematic view of lead compound **2** is docked to the crystal structure of 20S proteasome. (C) Lead compound **2** is depicted in the 20S proteasome active site. (D) Shown is the superposition of the three inhibitors compound **2**, homobelactosin **C**, and 2-spiro-lactacystin.

residue. Moreover, the CO-phenylalanine arm seems to be well superimposable to homobelactosin molecule, even with regard to the spatial disposition of N/O atoms.

The molecular docking studies suggest a nucleophilic attack from the N-terminal threonine residue of the β -subunits to the carbonyl group of compound **2** as a mechanism for proteasomal inhibition. To test whether the binding of compound **2** to the proteasome is reversible, we performed washout experiments in HeLa cells briefly treated with compound **2** or bortezomib, here used as reversible inhibitor positive control, and evaluated for residual cell viability. Our results (Supporting Information Figure 2) indicate that similar to bortezomib, compound **2** washout leads to a partial recovery in cell viability compared to nonwashout cultures. Taken together, this suggests that compound **2** is a covalent and reversible proteasome inhibitor.

Conclusion

In this report we have designed, synthesized, and defined the biological properties of a new series of chalcone-based compounds containing an α,β -unsaturated carbonyl system and bearing amino acid substitutions on the amino group of the 4-piperidone. The lead within this series, compound **2**, is an inhibitor of proteasomal function in vitro and in living cells, is

cell permeable, and acts upon all three known proteolytic activities in purified proteasomes. Nucleophilic susceptibility suggested by in silico docking studies conducted with compound **2** suggests that the α,β -unsaturated carbonyl system may represent the functional group for nucleophilic attack from the N-terminal threonine residue in the catalytic sites of the proteasome. Moreover, a single neutral amino acid substitution with tyrosine or leucine results in a decrease in the overall inhibition proteasome activity in all three known catalytic activities and reduced killing of HPV+ cervical cancer cells. Importantly, the different profile of proteasome inhibition of our lead compound **2** versus bortezomib results in synergistic killing of cervical cancers, indicating that simultaneous inhibition in cervical cancer cells of multiple proteasome activities results in a prerequisite for cervical cancer cells killing. These findings provide the rationale for combining compound **2** with bortezomib to potentially achieve broader proteasome inhibition and improved antitumor activity while possibly allowing for the use of lower doses of bortezomib to minimize toxic effects.

Experimental Section

General. All reagents and solvents were obtained from Aldrich. Anhydrous solvents were used as received. Reaction

progress was monitored with analytical thin-layer chromatography (TLC) carried out on 0.25 mm Merck F-254 silica gel glass plates. Visualization was achieved using UV illumination. ^1H NMR spectra were obtained at 400 MHz on a Bruker Avance spectrometer and are reported in parts per million downfield relative to tetramethylsilane (TMS). EI-MS profiles were obtained using a Bruker Esquire 3000 plus. All tested compounds were >95% purity as determined by a Waters HPLC system and one of the following methods, unless otherwise explicitly noted. Method 1 (at both 214 and 254 nm) used the following: semipreparative RP-HPLC column from Phenomenex, Luna C18, particle size 10 μm , 250 mm \times 10 mm with a flow rate of 1–6 mL/min with a gradient of 5–95% acetonitrile/water with 0.1% TFA over 30 min. Method 2 (at both 214 and 254 nm) used the following: semipreparative RP-HPLC column from Phenomenex, Luna C18, particle size 10 μm , 250 mm \times 10 mm with a flow rate of 1–6 mL/min with a gradient of 5–95% acetonitrile/water with 0.1% TFA over 40 min.

Chemistry. Synthesis of library compounds was based on Schemes 1 and 2. 3,5-Bis(arylidene)-4-piperidones **3** have been synthesized utilizing a Claisen–Schmidt condensation of 4-piperidone monohydrate hydrochloride **2**, and 3,4-dichlorobenzaldehyde **1** by passing dry HCl gas through a glacial acetic acid solution.³³ The AcOH salt of bischalcone **3** was treated with triethylamine to get free amine **4** (Scheme 1). *p*-Nitrochloroformate **5** was treated with the amine functionality of appropriate amino acid **6** bound to chlorotriptyl resin in the presence of *N,N*-diisopropylethylamine (DIEA) resulting in the formation of compound **7** (in situ) (Scheme 2) which has been further coupled to compound **4** in the presence of NMM, resulting in the formation of compound **8**, which then detached from the chlorotriptyl resin by using 20% trifluoroacetic acid, yielding the target compounds **2–10**. The dipeptides were synthesized using *tert*-butoxycarbonyl manual stepwise solid-phase peptide synthesis (SPPS) on chlorotriptyl resin using 2-(1*H*-benzotriazole-1-yl)-1,1,3,3-tetramethyluronium hexafluorophosphate (HBTU)/(DIEA).

Cell Culture. Cervical cancer cell lines HeLa, CaSki, SiHa, and ME180 were obtained from American Type Culture Collection (Manassas, VA) and cultured in DMEM supplemented with 10% fetal bovine serum, 100 IU/mL penicillin, and 100 μg /mL streptomycin at 5% CO_2 . Keratinocytes were obtained from Invitrogen (Carlsbad, CA) and cultured in defined keratinocyte-SFM.

Cell Viability Assay. Cell viability was determined by 2,3-bis-[2-methoxy-4-nitro-5-sulphophenyl]-2*H*-tetrazolium-5-carboxanilide inner salt (XTT) assay (Roche Diagnostics GmbH, Mannheim, Germany). Cells seeded at a concentration of 1000 per well in 100 μL of medium in a 96-well plate were treated with chalcone-based derivatives at specified concentrations. After the indicated periods, cells were incubated according to the manufacturer's protocol with the XTT labeling mixture for 4 h. Formazan dye was quantified using a spectrophotometric plate reader to measure the absorbance at 450 nm (ELISA reader 190; Molecular Devices, Sunnyvale, CA). All experiments were done in triplicate.

Plasmids. The plasmids p-CMV-FL and Ub-FL containing four tandem copies of ubiquitin G76V were a generous gift from Dr. D. Piwnicka-Worms (Washington University School of Medicine, St. Louis, MO).

Luciferase Assay. HeLa cells were cultured in DMEM medium with 10% heat-inactivated FBS, 1% glutamine, and 0.1% penicillin/streptomycin solution. The 2×10^5 cells per 6-well were transfected using effectine transfection reagent (Qiagen) with either p-CMV-FL or Ub-FL plasmids. Twenty-four hours after transfection, cells were transferred into 96-well plates at 1×10^4 cells/well in 100 μL of culture volume.

After cells were attached (18 h), the culture medium was replaced with 100 μL of medium containing drugs at the indicated concentrations. After 6 h of treatment, luciferase activity in cell lysate was determined with a luciferase assay kit (Promega). Values are calculated as relative luminescence units (RLU) and expressed as percent of control.

Cellular Morphology Analysis. A Leica DM IL LED inverted microscope was used for the imaging with phase contrast for cellular morphology.

In Vitro Effect of Proteasome Inhibitors. Cells (5×10^8) were washed in cold PBS and resuspended in buffer containing 50 mM Tris-HCl (pH 7.5), 5 mM MgCl_2 , 1 mM DTT (Sigma), 2 mM ATP, and 250 mM sucrose. Glass beads equivalent to the volume of the cell suspension were added, and the mixture was vortexed for 1 min at 4 $^\circ\text{C}$. Beads and cell debris were removed by 5 min of centrifugation at 1000g, followed by 20 min of centrifugation at 10000g.^{34,35} Lysates were cleared by ultracentrifugation for 1 h at 100000g, and supernatants were further ultracentrifuged for 5 h at 100000g. Proteasome-containing pellets were resuspended in 0.5 mL of homogenization buffer [50 mM Tris-HCl (pH 7.5), 100 mM KCl, 15% glycerol]. Protein concentration was determined using the BCA protocol (Pierce, Rockford, IL). Fluorogenic substrates Suc-LLVY-AMC, Boc-LRR-AMC, and Ac-YVAD-AMC were used to measure chymotryptic-like, tryptic-like, and caspase-like activities, respectively. Semipurified proteasomes were pretreated or not with inhibitors for 30 min at 37 $^\circ\text{C}$, were assayed at 37 $^\circ\text{C}$ for 45 min using the different peptide substrates in a buffer containing 50 mM Tris-HCl (pH 7.5), 5 mM MgCl_2 , and 1 mM DTT (final volume 100 L). The reaction was quenched with 1 mL of 1% SDS and fluorescence determined by a fluorimeter (Perkin-Elmer, Beaconsfield, U.K.) with excitation at 380 nm and emission at 440 nm. Data are expressed as the percent inhibition relative to untreated proteasomal preparations.

Docking Simulation. The equilibrium structure of compound **2** was obtained by DFT calculations at the PW91/DN level, using Dmol³ code of the Material Studio system program.³⁶ At first, the molecule was docked to the crystal structure of the yeast 20S proteasome in complex with the inhibitor homobactosin C covalently bound to the terminal threonine of the $\beta 5$ active site [PDB code: 3E47].³⁷ Then the molecule in the same conformation was docked to the crystal structure of 2-spiro-lactacystin/proteasome complex [PDB code: 3DY4].³⁸ The structures have been retrieved from the Protein Data Bank (PDB) archive (www.pdb.org), and the docking simulation has been performed using the MOE/Dock procedure integrated in the MOE system of programs (Chemical Computing Group Inc., MOE 2006.08). Before the simulation, hydrogen atoms were added to the inner part of the enzyme and the energy of the structure was minimized using the Amber99 molecular mechanics force field.³⁹ During the first step of the docking application, the ligand was treated in a flexible manner by rotating rotatable bonds and a number of the ligand's configurations were generated and scored in an effort to determine favorable binding modes by the application of the α triangle placement method. The ligand was docked restricting the search for binding modes to a specific, small region of the subunit called the $\beta 5$ -binding site, in which the terminal Thr1 is the active residue.

Statistical Analysis. Results are reported as the mean \pm standard error (SE). Statistical significance of differences was assessed by two-tailed Student's *t* test using Prism (version 5; GraphPad, San Diego, CA) and Excel. The level of significance was set at $p \leq 0.05$. The combination index (CI) of PS-341 and compound **2** was calculated by the median-effect analysis according to the method of Chou and Talaly.⁴⁰ $\text{CI} < 1$ indicates synergism, $\text{CI} = 1$ indicates additivity, and $\text{CI} > 1$ indicates antagonism. Further regression analyses were performed to stabilize estimates.

Acknowledgment. Grant support was provided by National Institutes of Health ATIP and SPOR in Cervical Cancer, Grant P50 CA098252 to S.R.K. and R.B.S.R., and the HERA Foundation to M.B. and B.K. We are thankful to Dr. David Piwnicka-Worms (Washington University School of Medicine, St. Louis, MO) for the generous gift of p-CMV-FL

and Ub-FL plasmids. M.K.R.M. is indebted to Department of Science and Technology, New Delhi, India, for their support (BOYSCAST Fellowship) to carry out this work at The Johns Hopkins University, Baltimore, MD.

Supporting Information Available: Synthesis details and analytical data of intermediates and products 2–10; specificity and reversibility data. This material is available free of charge via the Internet at <http://pubs.acs.org>.

References

- Ciechanover, A.; Finley, D.; Varshavsky, A. The ubiquitin-mediated proteolytic pathway and mechanisms of energy-dependent intracellular protein degradation. *J. Cell. Biochem.* **1984**, *24*, 27–53.
- Ciechanover, A. The ubiquitin-mediated proteolytic pathway. *Brain Pathol.* **1993**, *3*, 67–75.
- Orlowski, M.; Wilk, S. Catalytic activities of the 20 S proteasome, a multicatalytic proteinase complex. *Arch. Biochem. Biophys.* **2000**, *383*, 1–16.
- Bazzaro, M.; Lin, Z.; Santillan, A.; Lee, M. K.; Wang, M. C.; Chan, K. C.; Bristow, R. E.; Mazitschek, R.; Bradner, J.; Roden, R. B. Ubiquitin proteasome system stress underlies synergistic killing of ovarian cancer cells by bortezomib and a novel HDAC6 inhibitor. *Clin. Cancer Res.* **2008**, *14*, 7340–7347.
- Bazzaro, M.; Lee, M. K.; Zoso, A.; Stirling, W. L.; Santillan, A.; Shih, J. M.; Roden, R. B. Ubiquitin–proteasome system stress sensitizes ovarian cancer to proteasome inhibitor-induced apoptosis. *Cancer Res.* **2006**, *66*, 3754–3763.
- Curran, M. P.; McKeage, K. Bortezomib: a review of its use in patients with multiple myeloma. *Drugs* **2009**, *69*, 859–888.
- Fenical, W.; Jensen, P. R.; Palladino, M. A.; Lam, K. S.; Lloyd, G. K.; Potts, B. C. Discovery and development of the anticancer agent salinosporamide A (NPI-0052). *Bioorg. Med. Chem.* **2009**, *17*, 2175–2180.
- Kuhn, D. J.; Chen, Q.; Voorhees, P. M.; Strader, J. S.; Shenk, K. D.; Sun, C. M.; Demo, S. D.; Bennett, M. K.; van Leeuwen, F. W.; Chanan-Khan, A. A.; Orlowski, R. Z. Potent activity of carfilzomib, a novel, irreversible inhibitor of the ubiquitin–proteasome pathway, against preclinical models of multiple myeloma. *Blood* **2007**, *110*, 3281–3290.
- Genin, E.; Reboud-Ravaux, M.; Vidal, J. Proteasome inhibitors: recent advances and new perspectives in medicinal chemistry. *Curr. Top. Med. Chem.* **2010**, *10*, 232–256.
- Basse, N.; Montes, M.; Marechal, X.; Qin, L.; Bouvier-Durand, M.; Genin, E.; Vidal, J.; Villoutreix, B. O.; Reboud-Ravaux, M. Novel organic proteasome inhibitors identified by virtual and in vitro screening. *J. Med. Chem.* **2010**, *53*, 509–513.
- Kaiser, M.; Groll, M.; Renner, C.; Huber, R.; Moroder, L. The core structure of TMC-95A is a promising lead for reversible proteasome inhibition. *Angew. Chem., Int. Ed.* **2002**, *41*, 780–783.
- Kohno, J.; Koguchi, Y.; Nishio, M.; Nakao, K.; Kuroda, M.; Shimizu, R.; Ohnuki, T.; Komatsubara, S. Structures of TMC-95A-D: novel proteasome inhibitors from *Apiospora montagnei* sacc. TC 1093. *J. Org. Chem.* **2000**, *65*, 990–995.
- Laurent, N.; de Bouard, S.; Guillamo, J. S.; Christov, C.; Zini, R.; Jouault, H.; Andre, P.; Lotteau, V.; Peschanski, M. Effects of the proteasome inhibitor ritonavir on glioma growth in vitro and in vivo. *Mol. Cancer Ther.* **2004**, *3*, 129–136.
- Basse, N.; Papapostolou, D.; Pagano, M.; Reboud-Ravaux, M.; Bernard, E.; Felten, A. S.; Vanderesse, R. Development of lipopeptides for inhibiting 20S proteasomes. *Bioorg. Med. Chem. Lett.* **2006**, *16*, 3277–3281.
- Dick, L. R.; Fleming, P. E. Building on bortezomib: second-generation proteasome inhibitors as anti-cancer therapy. *Drug Discovery Today* **2010**, *15*, 243–249.
- Hawley-Nelson, P.; Vousden, K. H.; Hubbert, N. L.; Lowy, D. R.; Schiller, J. T. HPV16 E6 and E7 proteins cooperate to immortalize human foreskin keratinocytes. *EMBO J.* **1989**, *8*, 3905–3910.
- Reinstein, E.; Scheffner, M.; Oren, M.; Ciechanover, A.; Schwartz, A. Degradation of the E7 human papillomavirus oncoprotein by the ubiquitin–proteasome system: targeting via ubiquitination of the N-terminal residue. *Oncogene* **2000**, *19*, 5944–5950.
- Narisawa-Saito, M.; Kiyono, T. Basic mechanisms of high-risk human papillomavirus-induced carcinogenesis: roles of E6 and E7 proteins. *Cancer Sci.* **2007**, *98*, 1505–1511.
- Boulet, G.; Horvath, C.; Vanden Broeck, D.; Sahebali, S.; Bogers, J. Human papillomavirus: E6 and E7 oncogenes. *Int. J. Biochem. Cell Biol.* **2007**, *39*, 2006–2011.
- Achanta, G.; Modzelewska, A.; Feng, L.; Khan, S. R.; Huang, P. A boronic-chalcone derivative exhibits potent anticancer activity through inhibition of the proteasome. *Mol. Pharmacol.* **2006**, *70*, 426–433.
- Bonfili, L.; Cecarini, V.; Amici, M.; Cuccioloni, M.; Angeletti, M.; Keller, J. N.; Eleuteri, A. M. Natural polyphenols as proteasome modulators and their role as anti-cancer compounds. *FEBS J.* **2008**, *275*, 5512–5526.
- Cuccioloni, M.; Mozzicafreddo, M.; Bonfili, L.; Cecarini, V.; Eleuteri, A. M.; Angeletti, M. Natural occurring polyphenols as template for drug design. Focus on serine proteases. *Chem. Biol. Drug Des.* **2009**, *74*, 1–15.
- Milacic, V.; Banerjee, S.; Landis-Piowar, K. R.; Sarkar, F. H.; Majumdar, A. P.; Dou, Q. P. Curcumin inhibits the proteasome activity in human colon cancer cells in vitro and in vivo. *Cancer Res.* **2008**, *68*, 7283–7292.
- Mozzicafreddo, M.; Cuccioloni, M.; Bonfili, L.; Eleuteri, A. M.; Fioretti, E.; Angeletti, M. Antiplasmin activity of natural occurring polyphenols. *Biochim. Biophys. Acta* **2008**, *1784*, 995–1001.
- Bogyo, M.; Shin, S.; McMaster, J. S.; Ploegh, H. L. Substrate binding and sequence preference of the proteasome revealed by active-site-directed affinity probes. *Chem. Biol.* **1998**, *5*, 307–320.
- Kessler, B. M.; Tortorella, D.; Altun, M.; Kisselev, A. F.; Fiebig, E.; Hekking, B. G.; Ploegh, H. L.; Overkleeft, H. S. Extended peptide-based inhibitors efficiently target the proteasome and reveal overlapping specificities of the catalytic beta-subunits. *Chem. Biol.* **2001**, *8*, 913–929.
- Marastoni, M.; Baldisserotto, A.; Trapella, C.; Gavioli, R.; Tomatis, R. Synthesis and biological evaluation of new vinyl ester pseudotriptide proteasome inhibitors. *Eur. J. Med. Chem.* **2006**, *41*, 978–984.
- Baldisserotto, A.; Marastoni, M.; Fiorini, S.; Pretto, L.; Ferretti, V.; Gavioli, R.; Tomatis, R. Vinyl ester-based cyclic peptide proteasome inhibitors. *Bioorg. Med. Chem. Lett.* **2008**, *18*, 1849–1854.
- Chauhan, D.; Hideshima, T.; Anderson, K. C. Targeting proteasomes as therapy in multiple myeloma. *Adv. Exp. Med. Biol.* **2008**, *615*, 251–260.
- Baldisserotto, A.; Destro, F.; Vertuani, G.; Marastoni, M.; Gavioli, R.; Tomatis, R. N-terminal-prolonged vinyl ester-based peptides as selective proteasome beta1 subunit inhibitors. *Bioorg. Med. Chem.* **2009**, *17*, 5535–5540.
- Luker, G. D.; Pica, C. M.; Song, J.; Luker, K. E.; Pownica-Worms, D. Imaging 26S proteasome activity and inhibition in living mice. *Nat. Med.* **2003**, *9*, 969–973.
- Groll, M.; Huber, R. Purification, crystallization, and X-ray analysis of the yeast 20S proteasome. *Methods Enzymol.* **2005**, *398*, 329–336.
- McElvain, S. M.; McMahon, R. E. Piperidine derivatives. 4-piperidone, 4-piperidinol and certain of their derivatives. *J. Am. Chem. Soc.* **1949**, *71*, 3.
- Gavioli, R.; Vertuani, S.; Masucci, M. G. Proteasome inhibitors reconstitute the presentation of cytotoxic T-cell epitopes in Epstein–Barr virus-associated tumors. *Int. J. Cancer* **2002**, *101*, 532–538.
- Hendil, K. B.; Uerkevitz, W. The human multicatalytic proteinase: affinity purification using a monoclonal antibody. *J. Biochem. Biophys. Methods* **1991**, *22*, 159–165.
- Belley, B. Massive thermostats in isothermal density functional molecular dynamics simulations. *J. Chem. Phys.* **1990**, *50*, 1.
- Groll, M.; Larionov, O. V.; Huber, R.; de Meijere, A. Inhibitor-binding mode of homobactosin C to proteasomes: new insights into class I MHC ligand generation. *Proc. Natl. Acad. Sci. U.S.A.* **2006**, *103*, 4576–4579.
- Groll, M.; Balskus, E. P.; Jacobsen, E. N. Structural analysis of spiro beta-lactone proteasome inhibitors. *J. Am. Chem. Soc.* **2008**, *130*, 14981–14983.
- Ponder, J. W.; Case, D. A. Force fields for protein simulations. *Adv. Protein Chem.* **2003**, *66*, 27–85.
- Chou, T. C.; Talalay, P. Quantitative analysis of dose-effect relationship: the combined effects of multiple drugs or enzyme inhibitors. *Adv. Enzyme Regul.* **1984**, *22*, 27–55.